Technical Sciences
Academy of Romania
www.jesi.astr.ro

Journal of Engineering Sciences and Innovation
Volume 11, Issue 2 / 2026, pp. 135 - 148

A. Mechanical Engineering

Received ***04 December 2025*** *Accepted* ***11 May 2026***
Received in revised form ***20 Apryl 2026***

An analytical method of estimating the aerodynamic properties of airfoils on an extended range of angles of attack

MARIUS BREBENEL[1]*, CORNELIU BERBENTE[1], SORIN BERBENTE[2]

[1]National University of Science and technology POLITEHNICA of Bucharest, Romania
[2] INCDT-COMOTI, 220D Iuliu Maniu Blvd., Bucharest, Romania

Abstract. This paper proposes a new analytical method to determine the lift and drag coefficients of an airfoil at various angles of attack, including the post-stalled ones. The main objective is to allow the prediction of the behavior of bladed machines under conditions far from design (like propellers in reverse thrust or wind turbines at starting).
The lift and drag coefficients are estimated using new proposed analytical formulas, based on both aerodynamic theory and available test data. The plotted polars are compared to existing data (computed and experimental) and good similarities are observed. The analytical formulas provide also a way for a fast computation of propellers and wind turbines performances which need iterative operations involving aerodynamic coefficients of airfoils.

Keywords: lift, drag, polar, critical angle of attack (stall angle), optimum angle of attack.

1. Introduction

The analysis of the properties of aerodynamic airfoils is crucial in the design of aircraft, propellers, wind turbines and turbomachines. A propeller or wind turbine blade, for example, exhibits variations in the shape of the profile as well as angles of attack along it, initially unknown. As such, aerodynamic calculations involve knowledge of the properties of the airfoils (polars) in any section of the blade. Over time, the problem of polars has known both a theoretical and, above all, an experimental approach, so that, at present, there is a consistent database comprising polars determined in wind tunnels. However, in the design of bladed machines, an automation of calculations is necessary that cannot be done by "reading" experimental results. Such analytical methods are needed that lead to results consistent with experimental measurements, but which can be implemented in various computational application programs.

*Correspondence address: mariusbreb@yahoo.com

It should also be noted that, in recent years, a series of specific software for airfoils have been developed (such as Qblade, Xfoil, Rfoil) that can be used as a basis for comparison with more accessible analytical methods in the design of bladed machines (which involve computational iterations that predict initially unknown incidences). However, some programs (Xfoil) do not cover the entire incidence range of interest for the present work [-90°, 90°].

The problem of aerodynamic properties of airfoils has been addressed since the beginning of the 20th century, with the appearance of the first airplanes. We can thus recall the remarkable works of specialists in *Aerodynamics* such as L. Prandtl [1] (1921), L. M. Milne-Thompson [2] (1958) or F.W. Riegels [3] (1958), to mention only a few names in this regard. The cited authors laid the foundations of the analytical calculation of airfoils in simplifying hypotheses, such as potential flows in the presence of vortices that generate lift. It is obvious that in the adopted hypotheses, the critical angle of attack (stall incidence) could not be determined, nor the behavior of airfoils at higher incidences, as proposed in this article. Analytical approaches to airfoil properties on extended domains beyond the critical incidence have recently appeared in the works of authors D.A. Spera [4], [5] (2008 – 2009) or L. Battisti and Coll. [6] (2020). The formulas proposed by these authors are based on empirical correlations that give results close to the measured values. This article proposes calculation relations that start from classical *Aerodynamics* in the range up to the critical incidence and are extended by relations that also start from physical flow conditions, but are adjusted to be in agreement with the experimental data. Based on the proposed relations, the polars $c_L = f(\alpha)$, $c_D = f(\alpha)$, $c_L = f(c_D)$ will be determined on the range $\alpha \in [-90°, 90°]$ as well as the values $(c_L)_{\max}$, $(c_L / c_D)_{\max}$ and $\alpha_{opt} \mid c_L / c_D = \max$. These will then be compared with the results given by the currently used software as well as with the experimentally determined polars, available in the literature.

2. Calculation assumptions

It is obvious that the aerodynamic properties of airfoils are the effect of the complexity of the flow around them, so that a general method that encompasses all aerodynamic aspects is difficult to implement in application programs. For example, using *CFD* (Computational Fluid Dynamics) software, it is possible to analyze the flow around a given airfoil under any conditions, but this is difficult to introduce into an application such as the calculation of propeller blades or wind turbines, due to the initial lack of knowledge of the incidences at each section of the blade. Consequently, it is necessary to introduce some simplifying hypotheses in order to develop a mathematical model that is easy to implement in specific calculation programs. We present these hypotheses below:

1) The profiles are considered 2D (respectively as for a wing with infinite span);
2) The influence of the Reynolds number is neglected (Re = 200000 will be considered as reference for comparisons with other results from the literature);
3) The influence of the profile thickness is neglected;

4) The compressibility effects are not considered;
5) The polar is the result of the superposition of the lift and drag effects;
6) The critical incidence will be taken as a universal value α_{cr} = 15° for simple profiles, without flaps. Airfoils with flaps are not the subject of this study;
7) In the neighborhood of the incidence $\alpha = 0$ the result of classical *Aerodynamics* will be considered, respectively

$$c_L(\alpha) = 2\pi(\alpha + \tau) \tag{1}$$

where τ = the camber angle of the airfoil (in radians) given by

$$\tau = \arctan(2\bar{f}) \tag{2}$$

$\bar{f}$ = the maximum relative camber line deflection.

3. Analysis of the lift effect

At low incidences and in the case of slightly cambered profiles, the effect of circulation around the profile is manifested in the domain. This assumes that the downstream wake starts from the trailing edge level, which is equivalent to the existence of a circulation Γ around the profile which, according to the Kutta-Jukowski theorem, generates the lift force perpendicular to the direction of the incident velocity:

$$\vec{L} = \rho \vec{V}_\infty \times \vec{\Gamma} \tag{3}$$

Since the increase in the angle of attack leads to the appearance of detachments on the suction side, the circulation gradually decreases and at a given moment the lift begins to decrease. As such, the linear variation of the lift coefficient is limited, the respective coefficient reaching a maximum value at the incidence called critical in the case of any aerodynamic profile. Under these conditions, a sinusoidal variation of the lift coefficient of the form:

$$c_L(\alpha) = (c_L)_{\max} \sin\left(\frac{\pi}{2}\frac{\alpha + \tau}{\alpha_{cr} + \tau}\right) \tag{4}$$

is proposed so that, when reaching the critical incidence, the lift coefficient reaches its maximum value:

$$\alpha = \alpha_{cr} \Rightarrow c_L = (c_L)_{\max}. \tag{5}$$

The maximum value of the lift coefficient is determined by setting the condition that at zero incidence, the slope of the polar given by equation (4) coincides with that given by the classical theory of thin profiles (1):

$$\alpha = 0 \quad \Rightarrow \quad \frac{dc_L}{d\alpha} = 2\pi \tag{6}$$

By differentiating expression (4) with respect to α and applying condition (6), we obtain:

$$\left.\frac{dc_L}{d\alpha}\right|_{\alpha=0} = (c_L)_{\max}\frac{\pi}{2}\frac{1}{\alpha_{cr}+\tau}\cos\left(\frac{\pi}{2}\frac{\alpha+\tau}{\alpha_{cr}+\tau}\right)\Bigg|_{\alpha=0} = (c_L)_{\max}\frac{\pi}{2}\frac{1}{\alpha_{cr}+\tau}\cos\left(\frac{\pi}{2}\frac{\tau}{\alpha_{cr}+\tau}\right) = 2\pi$$

$$(c_L)_{\max} = \frac{4(\alpha_{cr} + \tau)}{\cos\left(\frac{\pi}{2}\frac{\tau}{\alpha_{cr} + \tau}\right)} \tag{7}$$

Consequently, in the domain $|\alpha| \le \alpha_{cr}$, the proposed variation for c_L will be of the form:

$$c_L(\alpha) = \frac{4(\alpha_{cr} + \tau)}{\cos\left(\frac{\pi}{2}\frac{\tau}{\alpha_{cr} + \tau}\right)} \sin\left(\frac{\pi}{2}\frac{\alpha + \tau}{\alpha_{cr} + \tau}\right). \tag{8}$$

It should be noted that the decreasing portion of the polar generated by expression (8) is limited to the level at which the resistive effect begins to manifest.

4. Analysis of the drag effect

It is known that for a 2D flat plate (infinite length) placed perpendicular to the direction of the flow, the aerodynamic drag coefficient is $c_D = 2$ (fig. 1-a). In this case, the aerodynamic drag force results in:

$$D = c_D \frac{\rho}{2} V_\infty^2 b = \rho V_\infty^2 b \tag{9}$$

where b = chord of the profile. Assuming that, on the inclined plane plate (fig. 1-b), the aerodynamic drag occurs in exactly the same way, but with the velocity component perpendicular to the plate, one yields for the force on the plate:

$$F = \rho V_\infty^2 b \sin^2 \alpha . \tag{10}$$

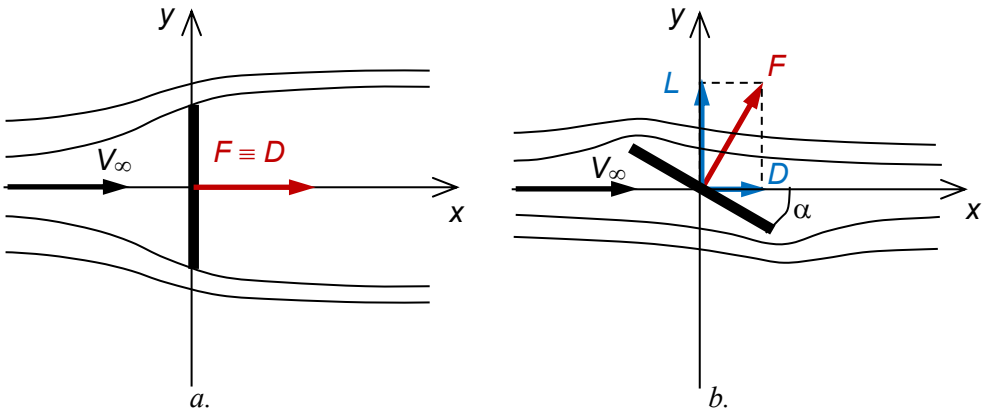

Fig. 1. Development of aerodynamic forces on a flat plate placed perpendicular to the direction of the flow (a) and with incidence (b).

By projecting the force F onto the x and y directions, the expressions for lift and aerodynamic drag are obtained according to their standard definitions:

$$L=\rho V_\infty^2 b\sin^2\alpha\cos\alpha,\ D=\rho V_\infty^2 b\left|\sin^3\alpha\right| \tag{11}$$

The corresponding dimensionless coefficients will be:

$$c_L(\alpha)=2\sin^2\alpha\cos\alpha,\ c_D(\alpha)=2\left|\sin^3\alpha\right| \tag{12}$$

However, experience shows that, for slightly cambered profiles (including flat plates), the coefficients due to the drag effect are better modeled by the formulas:

$$c_L(\alpha)=2\sin\alpha\cos\alpha=\sin 2\alpha,\ c_D(\alpha)=2\sin^2\alpha \tag{13}$$

5. Determination of the lift polar

Analyzing the proposed relations for the variation of the coefficient c_L with the angle of attack α, we deduce that the shape of the polar $c_L=f(\alpha)$ results from the superposition of two sinusoids: (8) and (13). Thus, by considering the two effects (lift and drag), the polar of the lift coefficients of the aerodynamic profiles will look like in Fig. 2:

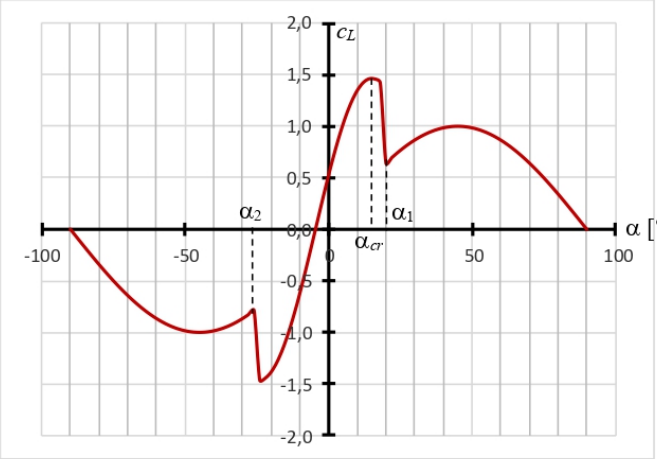

Fig. 2. Specific polar pattern of a slightly cambered profile.

Let α_1 and α_2 be the values of incidences at which the two sinusoidal curves intersect and α_{cr} the positive critical incidence, respectively. Introducing the characteristic function of an interval

$$\chi_{[a,b]}(x)=\begin{cases}1 & x\in[a,b]\\ 0 & \text{rest}\end{cases} \tag{14}$$

the polar represented in Fig. 2 can be described analytically by the expression:

$$c_L(\alpha)=\chi_{[\alpha_2,\alpha_1]}(\alpha)\frac{4(\alpha_{cr}+\tau)}{\cos\left(\frac{\pi}{2}\frac{\tau}{\alpha_{cr}+\tau}\right)}\sin\left(\frac{\pi}{2}\frac{\alpha+\tau}{\alpha_{cr}+\tau}\right)+\left[1-\chi_{[\alpha_2,\alpha_1]}(\alpha)\right]\sin 2\alpha \tag{15}$$

where, according to the figure, $\alpha_2 < \alpha_1$ and $\alpha \in \left[-\frac{\pi}{2}, \frac{\pi}{2}\right]$.

The characteristic function can also be written using the "sign" function (signum):

$$\chi_{[a,b]}(x) = \frac{1}{2}\left[\operatorname{sgn}(x-a) - \operatorname{sgn}(x-b)\right] \tag{16}$$

For the complete determination of the analytical expression of the polar, the values of the quantities α_1 and α_2 remain to be calculated.

We note:

$$f_1(\alpha) = \frac{4(\alpha_{cr}+\tau)}{\cos\left(\frac{\pi}{2}\frac{\tau}{\alpha_{cr}+\tau}\right)} \sin\left(\frac{\pi}{2}\frac{\alpha+\tau}{\alpha_{cr}+\tau}\right) \qquad f_2(\alpha) = \sin 2\alpha \tag{17}$$

The equation $f_1(\alpha) = f_2(\alpha)$ is transcendental, but does not present any particular difficulties in being solved numerically. However, a difficulty arises when we want to quickly find the two solutions in the interval $\alpha \in \left[-\frac{\pi}{2}, \frac{\pi}{2}\right]$, that is α_1 and α_2 (hereinafter called ***reference incidences***).

A simplification in this sense can be applied based on the observation that the two solutions of the equation are very close to the solutions of the equation

$$f_3(\alpha) = \sin 2\alpha \quad \text{where} \quad f_3(\alpha) = \sin\left(\frac{\pi}{2}\frac{\alpha}{\alpha_{cr}+\tau}\right) \tag{18}$$

especially in the area of positive values of incidence. In fig. 3 and 4 the 3 curves defined by the expressions $f_1(\alpha)$, $f_2(\alpha)$ and $f_3(\alpha)$ for 2 airfoils with the maximum relative camber line deflection $\bar{f} = 0{,}01$ and $\bar{f} = 0{,}04$ respectively, are graphically represented.

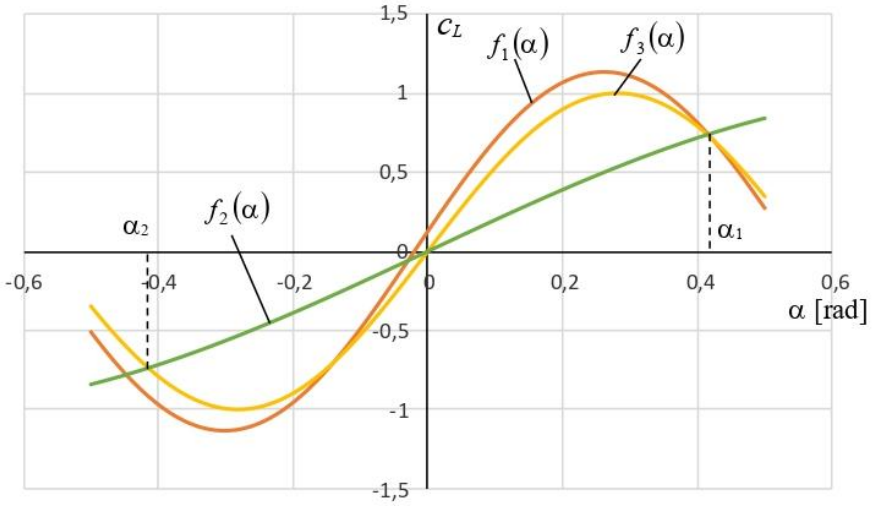

Fig. 3. Determination of reference incidences for an airfoil with $\bar{f} = 0{,}01$.

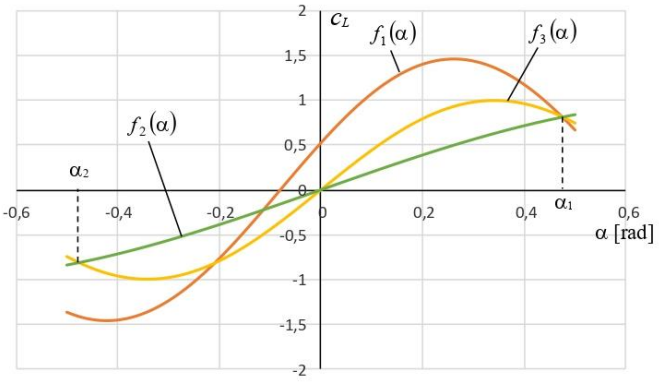

Fig. 4. Determination of reference incidences for an airfoil with $\bar{f} = 0{,}04$.

To solve equation (18), the classical trigonometric formulas will be used:

$$\sin\left(\frac{\pi}{2}\frac{\alpha}{\alpha_{cr}+\tau}\right)-\sin 2\alpha=0 \;\Rightarrow\; 2\sin\left(\frac{\pi}{4}\frac{\alpha}{\alpha_{cr}+\tau}-\alpha\right)\cos\left(\frac{\pi}{4}\frac{\alpha}{\alpha_{cr}+\tau}+\alpha\right)=0 \tag{19}$$

From the cancellation of the sine it follows:

$$\sin\left(\frac{\pi}{4}\frac{\alpha}{\alpha_{cr}+\tau}-\alpha\right)=0 \;\Rightarrow\; \alpha\left(\frac{\pi}{4}\frac{1}{\alpha_{cr}+\tau}-1\right)=0 \text{ or } \alpha\left(\frac{\pi}{4}\frac{1}{\alpha_{cr}+\tau}-1\right)=\pi \tag{20}$$

The solutions:

$$\alpha=0 \quad \text{or} \quad \alpha=\frac{\pi}{\frac{\pi}{4}\frac{1}{\alpha_{cr}+\tau}-1} \tag{21}$$

do not agree. We analyze the solutions resulting from cosine cancellation:

$$\cos\left(\frac{\pi}{4}\frac{\alpha}{\alpha_{cr}+\tau}+\alpha\right)=0 \Rightarrow \alpha_1\left(\frac{\pi}{4}\frac{\alpha}{\alpha_{cr}+\tau}+1\right)=\frac{\pi}{2} \text{ or } \alpha_2\left(\frac{\pi}{4}\frac{\alpha}{\alpha_{cr}+\tau}+1\right)=-\frac{\pi}{2} \tag{22}$$

$$\alpha_{1,2}=\pm\frac{2\pi(\alpha_{cr}+\tau)}{\pi+4(\alpha_{cr}+\tau)}. \tag{23}$$

With the reference incidence values thus determined, formula (15) satisfactorily models the polar $c_L=f(\alpha)$ over the entire domain $\alpha\in\left[-\frac{\pi}{2},\frac{\pi}{2}\right]$ as it can observe from the comparison with the experimental polar patterns.

6. Determination on the drag polar

For the variation of the aerodynamic drag coefficient $c_D=f(\alpha)$, we will start from formula (13) which will be corrected in the form:

$$c_D(\alpha) = c_{D0} + 2\sin^2(\alpha - \alpha_m) \tag{24}$$

where, by α_m we denoted the ***ideal angle of attack*** (that is the one at which c_D is minimum). Consequently, the coefficient c_D will depend on 2 parameters: its minimum value c_{D0} and the incidence at which this minimum occurs, that is α_m.
It is known that the minimum value of the coefficient c_D is an effect of the boundary layer and, as such, depends on the Reynolds number:

$$c_{D0} = f(\mathrm{Re}) \tag{25}$$

For a flat plate in turbulent regime, classical theory provides the formula [8]:

$$c_{D0} = \frac{0{,}148}{\mathrm{Re}_L^{1/5}} \quad \text{for} \quad \mathrm{Re}_L < 10^7 \tag{26}$$

where the subscript $[\,]_L$ refers to the length of the plate.
However, it is observed from the experimental data that, in general, the magnitude of the coefficient c_{D0} in turbulent regime for slightly cambered airfoils oscillates around the value

$$c_{D0} \cong 0{,}007 \tag{27}$$

which can be taken as a datum for most common airfoils. The ideal incidence (denoted by α_m) depends on the shape of the airfoil camber line. Thus, for an airfoil with a camber line of equation

$$y_s = y_s(x), \quad x \in [0,1] \tag{28}$$

the classical theory of *Aerodynamics* provides the formula:

$$\alpha_m = \frac{1}{\pi}\int_0^{\pi} \frac{dy_s}{dx} \cdot d\theta \ \ [\mathrm{rad}] \tag{29}$$

where

$$x = \frac{1}{2}(1 + \cos\theta) \tag{30}$$

Example: For an airfoil with a parabolic camber line equation

$$y_s = 4\bar{f}x(1 - x) \tag{31}$$

whose maximum relative camber is $\bar{f}$, it is found:

$$\frac{dy_s}{dx} = 4\bar{f}(1 - 2x) = -4\bar{f}\cos\theta \tag{32}$$

$$\alpha_m = \frac{1}{\pi}\int_0^{\pi} (-4\bar{f})\cos\theta \cdot d\theta = 0 \tag{33}$$

It can be shown that for any airfoil with a symmetrical camber line about its center, the ideal angle of attack is zero. For airfoils with an asymmetrical camber line, the angle α_m is different from zero, but not by much, so that, as a first approximation, we can consider in calculations $\alpha_m \cong 0$ for most common airfoils. Consequently, the aerodynamic drag coefficient c_D can be approximated by the formula:

$$c_D(\alpha) = 0{,}007 + 2\sin^2\alpha\,, \quad \text{where} \quad \alpha \in \left[-\frac{\pi}{2}, \frac{\pi}{2}\right] \tag{34}$$

valid for any slightly cambered airfoil.

7. Determination of maximum value of (C_L/C_D)

The analytical expression of the aerodynamic coefficients c_L and c_D allows the determination of the maximum value of the ratio c_L / c_D. Using formulas (15) and (34), one yields:

$$\frac{c_L}{c_D}(\alpha) = \frac{4(\alpha_{cr} + \tau)}{\cos\left(\frac{\pi}{2}\frac{\tau}{\alpha_{cr} + \tau}\right)} \sin\left(\frac{\pi}{2}\frac{\alpha + \tau}{\alpha_{cr} + \tau}\right) \frac{1}{0{,}007 + 2\sin^2\alpha}\,, \tag{35}$$

with the remark that, in his expression, only the portion up to the stall incidence was considered, since the maximum value of the ratio c_L / c_D occurs at low incidences. By applying the condition of maximum, the following relations are successively derived:

$$\frac{d}{d\alpha}\left(\frac{c_L}{c_D}\right) = 0 \quad \Rightarrow \quad \frac{d}{d\alpha}\left[\sin\left(\frac{\pi}{2}\frac{\alpha + \tau}{\alpha_{cr} + \tau}\right)\frac{1}{0{,}007 + 2\sin^2\alpha}\right] = 0 \tag{36}$$

$$\frac{\pi}{2(\alpha_{cr} + \tau)}\cos\left(\frac{\pi}{2}\frac{\alpha + \tau}{\alpha_{cr} + \tau}\right)(0{,}007 + 2\sin^2\alpha) - 4\sin\alpha\cos\alpha\sin\left(\frac{\pi}{2}\frac{\alpha + \tau}{\alpha_{cr} + \tau}\right) = 0 \tag{37}$$

$$\frac{\pi}{2(\alpha_{cr} + \tau)}\left(\frac{0{,}007 + 2\sin^2\alpha}{\sin\alpha\cos\alpha}\right) - 4\,\mathrm{tg}\left(\frac{\pi}{2}\frac{\alpha + \tau}{\alpha_{cr} + \tau}\right) = 0 \tag{37}$$

By denoting with α_f the convenient solution of the above equation (numerically calculable), we will have:

$$\alpha = \alpha_f \quad \Rightarrow \quad \frac{c_L}{c_D} = \max \tag{38}$$

8. Comparative examples

Next, we will give some examples of aerodynamic polars calculated with the proposed formulas, compared with results given by Xfoil software and experimental diagrams.

1) Symmetrical airfoil NACA 0012

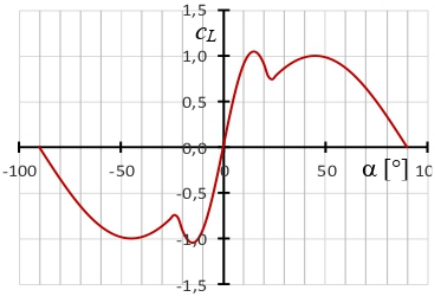

Fig. 5-a

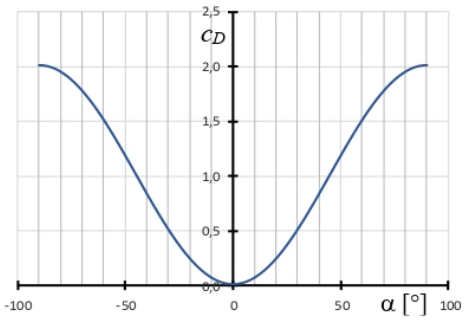

Fig. 5-b

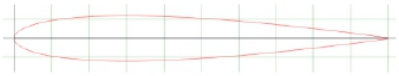

Re = 200000

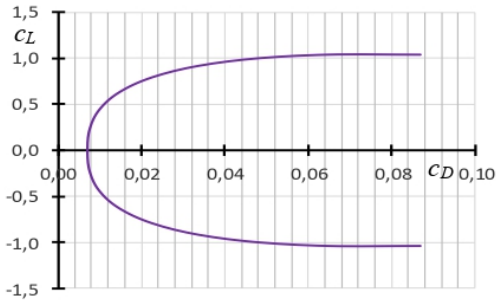

Fig. 5. Polars for airfoil NACA 0012 determined with proposed formulas $(C_L/C_D)_{max} = 25{,}93$ at $\alpha = 3°$.

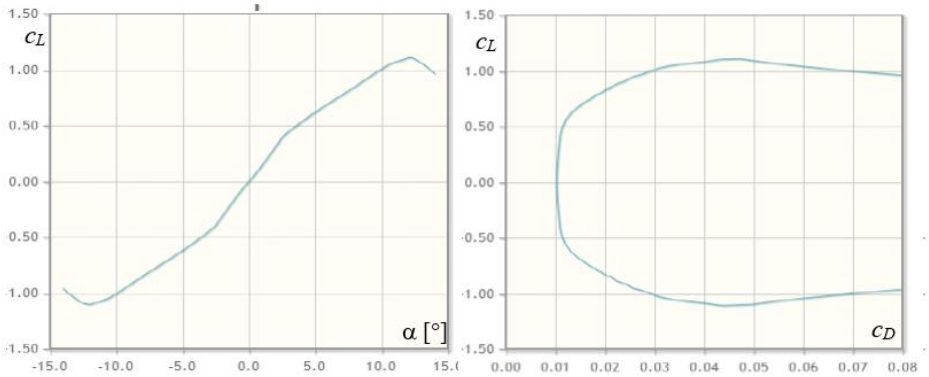

Fig. 6. Polars airfoil NACA 0012 determined by Xfoil - $(C_L/C_D)_{max} = 47{,}43$ at $\alpha = 5°$.

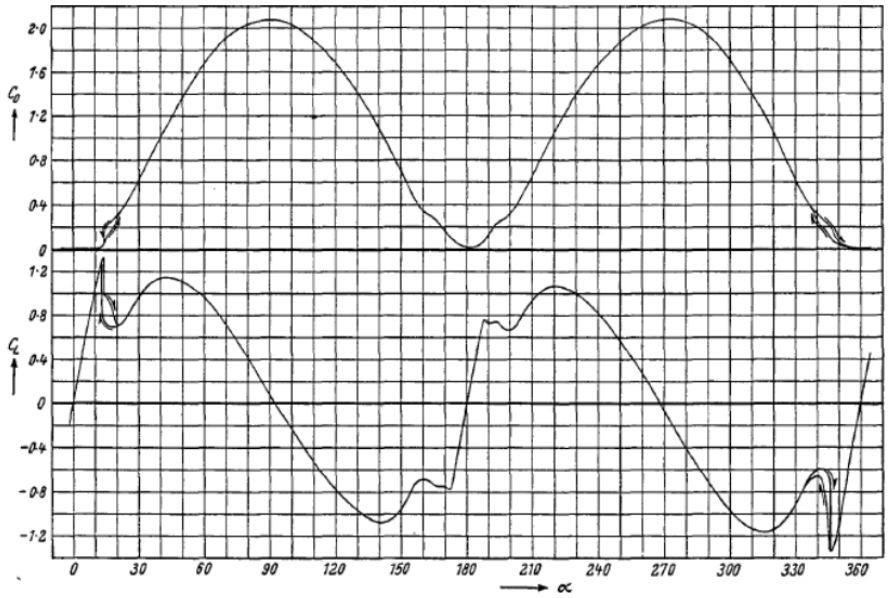

Fig. 7. Polars airfoil NACA 0012 determined experimentally [3]
$(C_L/C_D)_{max}$ = 42,86 at α = 3°

2) Cambered airfoil NACA 4418

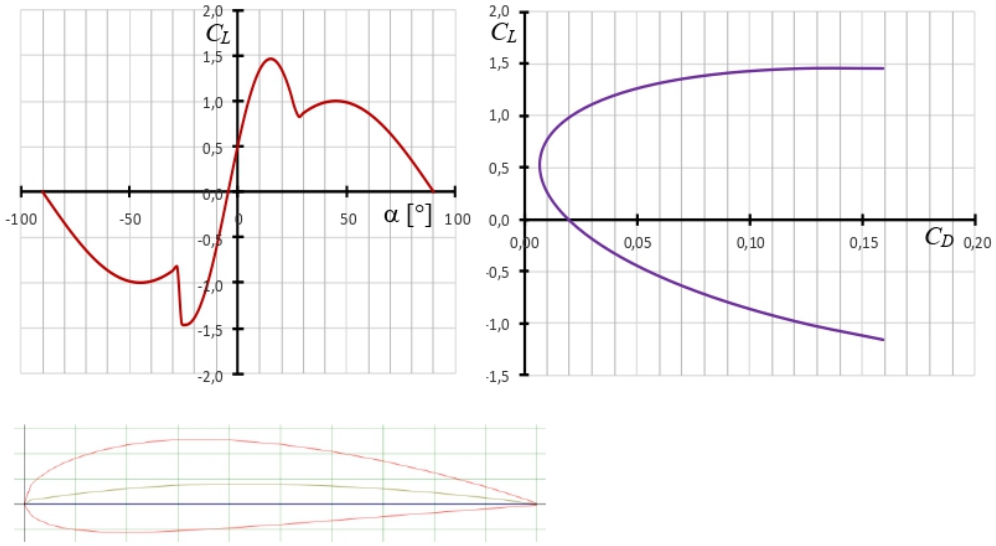

Fig. 8. Polars airfoil NACA 4418 determined with proposed formulas
$(C_L/C_D)_{max}$ = 78,11 at α = 2°.

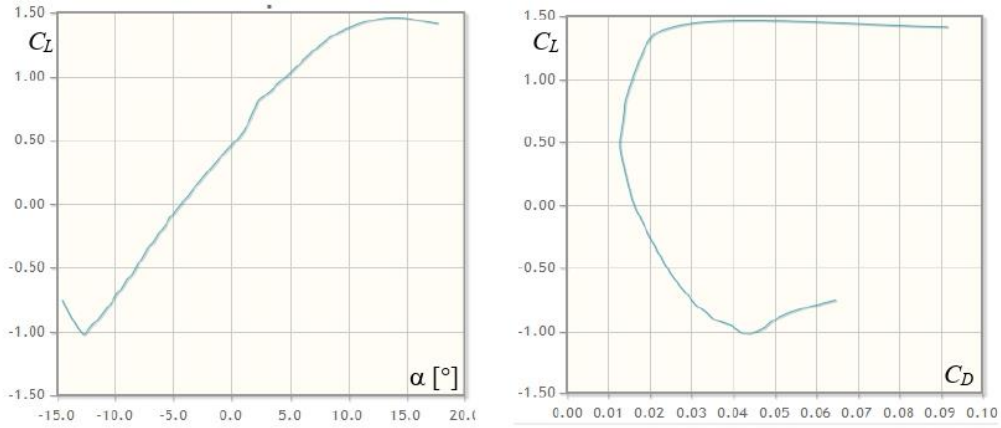

Fig. 9. Polars airfoil NACA 4418 determined by Xfoil
$(C_L/C_D)_{max}$ = 67,02 at α = 7,5°.

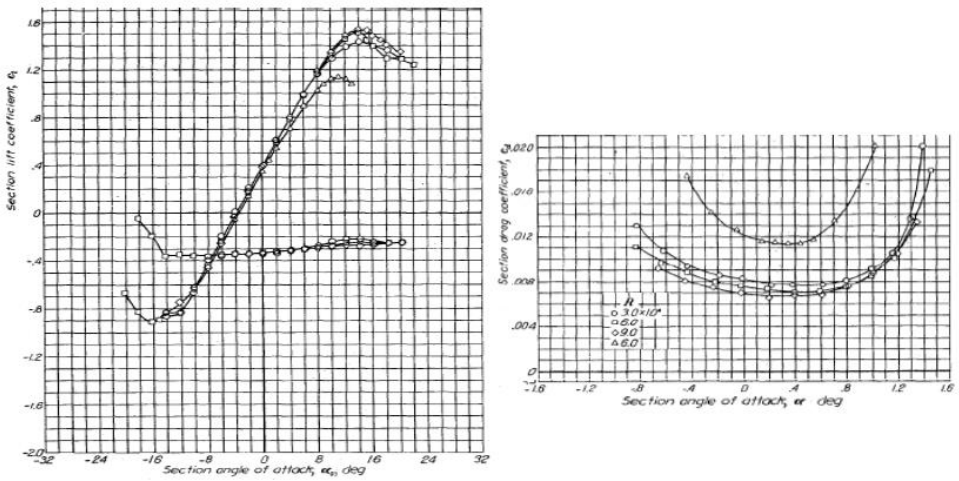

Fig. 10. Polars airfoil NACA 4418 determined experimentally [7]
$(C_L/C_D)_{max}$ = 64,28 at α = 4°

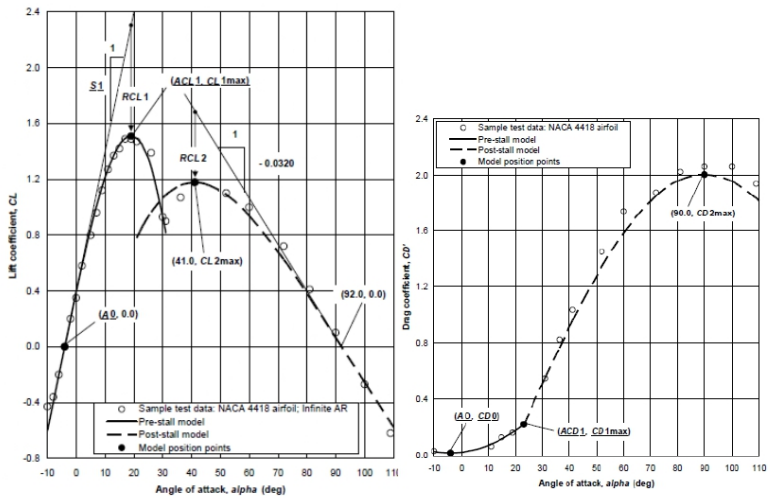

Fig. 11. Polars airfoil NACA 4418 determined theoretically by method *AERODAS* [4]
$(C_L/C_D)_{max}$ = 75,3 at α = 2,5°.

9. Findings on comparative examples

The polars of a symmetrical profile (NACA 0012) and of a cambered profile (NACA 4418 with maximum relative camber line deflection $\bar{f} = 0{,}04$) were compared. From the graphs represented, it can be observed a good agreement of the drag coefficient c_D predicted by formula (34) with both experimental and theoretical values given by other methods (such as the Xfoil or AERODAS method presented in [4] and illustrated in fig. 11). It is worth noting that the polars $c_D = f(\alpha)$ on the domain $\alpha \in [-90°, 90°]$ do not depend on the shape of the profile, at least within the admitted hypotheses. Regarding the variation of the lift coefficient c_L, a very good approximation can be observed between the results given by formula (15) and those given by Xfoil, AERODAS and the experimental data, especially in the domain up to the critical incidence, including the maximum lift. In the range of incidences higher than the critical one, some differences appear regarding the value of the second maximum of c_L, which according to the proposed method has the value $(c_L)^{(2)}_{max} = 1$ regardless of the profile shape or Reynolds number, while the experimental data show an obvious variation with the Reynolds number. It should be noted, however, that this second maximum for c_L appears for all profiles at an incidence of 45°, both in the proposed model and in the literature data. A similar situation occurs in the case of $(c_D)_{max}$ obtained at $\alpha = 90°$ and has the value 2. However, taking into account that the operation of an aerodynamic profile under these conditions is undesirable or transient and that the differences in numerical values are not too large, we consider the results of the proposed method to be acceptable. A questionable precision is obtained in the case of the maximum value of c_L/c_D which, in fact, exhibits a large dispersion of the values provided by different

sources, both theoretical and experimental. A synthesis of the above results is presented in table 1.

10. Conclusions

In this paper, new analytical calculation formulas for the characteristics of simple aerodynamic profiles (without flaps) have been proposed, for use in complex programs for the analysis of propellers and wind turbines. The new formulas allow the estimation of the aerodynamic characteristics of profiles over extended ranges of flow incidences, thus including the range of incidences higher than the critical one. Although the flow around airfoils under such conditions is quite complex, the proposed formulas lead to results that are satisfactorily close to those given by more complicated methods (*CFD*, *AERODAS*) or experimental ones. Analyzing a symmetric profile (NACA 0012) and a cambered one (NACA 4418), we find a good approach of the results given by the proposed method and those provided by other sources over the entire incidence range, thus allowing implementation in complex simulations without high consumption of computational resources.

Table 1. Comparison between the values calculated with the proposed model and those found in the literature regarding the characteristics of NACA 0012 and NACA 4418 airfoils.

Airfoil	**NACA 0012**				**NACA 4418**			
	Analytic	**Xfoil**	**Experim.**	**AERODAS**	**Analytic**	**Xfoil**	**Experim.**	**AERODAS**
$(c_L)^{(1)}_{\max}$	1,04	1,11	1,0	–	1,46	1,46	1,45	1,52
α_{cr}	15°	12,25°	13°	–	15°	16,25°	15°	18°
$(c_L)^{(2)}_{\max}$	1,0	–	1,17	1,173	1,0	–	–	1,18
$(c_L)_{\alpha=0}$	0	0	0	0	0,525	0,459	0,4	0,4
$(c_D)_{\min}$	0,007	0,010	0,010	–	0,007	0,013	0,007	0,003
$(c_D)_{\max}$	2	–	2,08	2,053	2	–	–	2
$(c_L / c_D)_{\max}$	25,93	47,43	42,86	–	78,11	67,02	64,28	75,3
$\alpha\|_{c_L/c_D=\max}$	3°	5°	3°	–	2°	7,5°	4°	2,5°

References

[1] Prandtl L., *Applications of Modern Hydrodynamics to Aeronautics*, NACA TR-116, June 1921.
[2] Milne-Thompson L. M., *Theoretical Aerodynamics*, Dover, New York, 1958.
[3] Riegels F.W., *Aerodynamische Profile*, Verlag R. Oldenbourg, Munich, 1958.
[4] Spera D.A., *Models of Lift and Drag Coefficients of Stalled and Unstalled Airfoils in Wind Turbines and Wind Tunnels*, NASA/CR – 2008-215434.
[5] Spera D.A., *Wind Turbine Technology*, ASME Press, New York, USA, 2009.
[6] Battisti L., Zanne L., Castelli M.R., Bianchini A., Brighenti A., *A generalized method to extend airfoil polars over the full range of angles of attack*, Renewable Energy, **155**, 2020, p. 862-875.
[7] Abbott I.H., Von Doenhoff A.E., Stivers L.S. Jr., *Summary of airfoil data*, NACA Report No. 824, 1945.
[8] Constantinescu V.N., Găletuşe S., *Mecanica Fluidelor şi Elemente de Aerodinamică*, Ed. Didactică şi Pedagogică, Bucureşti, 1983.